Depth migration of monostatic and bistatic georadar data

Robert J. Ferguson, Matthew J. Yedlin, Christian Pichot, Jean-Yves Dauvignac, Nicholas Fortino, and Stephane Gaffet

ABSTRACT

A 200 trace subset of a larger survey conducted in the "aniti-blast" tunnel of the Inter-Disciplinary Underground Science & Technology Laboratory are compared for image quality. These data are unique in that two distinct acquisition geometries are acquired simultaneously. The first, and we will call it "bistatic", is the conventional georadar acquisition where the transmitting and recording antennae are separated by 65 cm. The second we will call "monostatic". Monostatic acquisition is unique in that the transmitting and recording antennae are exactly co-located - they are the same physical antenna, and this is a recent technical development. Monostatic acquisition reproduces exactly the geometry of the well known "exploding reflector model" of seismic imaging and therefore, zero-offset migration (ZOM) of the data is not an approximation but a legitimate imaging approach. In particular, the image of the near-surface (1 m or so) should be precisely imaged (given an exact velocity model) - bistatic data require prestack depth migration (PSDM) to achieve equal precision. PSDM, of course, is much more expensive and time consuming than ZOM and so monostatic acquisition is very desirable. Here we demonstrate a number of important differences.

INTRODUCTION

Georadar data were acquired in March 2011 in the anti-blast tunnel within the Inter-Disciplinary Underground Science & Technology Laboratory at the Laboratoire Souterrain á Bas Bruit (LSBB, http://lsbb.oca.eu), Rustrel, France (Yedlin et al., 2010). Georadar data are acquired at LSBB in experiments on detecting water content by mapping permittivity over depths of several metres. One of the most interesting technical aspects of the recordings is the use of both a conventional bistatic recording geometry (the source / receiver offset is about 65 cm) and what we will call a monostatic recording geometry where the emitting antenna is also the receiving antenna. The monostatic data correspond precisely to the exploding reflector model of seismic migration (Ferguson et al., 2010). This correspondence means that zero-offset migration (ZOM) should return a very good image of the subsurface for a low computational effort. In contrast, bistatic acquisition should be migrated using a prestack or constant offset method (Ferguson et al., 2010) - in particular for the shallow section.

In this paper, we compare migration images for ZOM of the monostatic data to ZOM of the bistatic data and prestack depth migration (PSDM) of the bistatic data. We proceed first through a Gabor-domain deconvolution procedure to reverse the amplitude and phase effects of Q attenuation (for details of the Gabor process please see Ferguson and Margrave 2012 this issue) to depth-variable velocity analysis using a modified depth migration algorithm. We find that there are a minimum of two distinct velocity zones - one shallow (0 - 5 m depth) with $\alpha = 0.2 \times c$ m/s where α is the measured georadar velocity and $c = 3 \times 10^8$ m/s. Note, all α values quoted are "half velocities" as in ZOM applications. For PSDM

they are doubled. The second zone extends from 5 m downward at $\alpha = 0.27 \times c$ m/s.

The migrated images show that ZOM of the monostatic data returns a very clean image of a number of shallow diffractors and layers that ZOM migration of the bistatic data images with less clarity. We find that PSDM of the bistatic data returns a marginally sharper image. Our findings are consistent in the deeper section with the exception that ZOM of the bistatic data is comparatively noisier that in the shallow section.

Computationally, we find that PSDM is much more expensive to run than ZOM by a factor that is $\propto N \log_2 N / \log_2 M$ where M is the number of traces and N is the number of traces that we pad around a single bistatic trace prior to PSDM (Ferguson et al., 2010). For $M = 256$ and $N = 128$, we find that PSDM is $\sim 100\times$ as expensive as ZOM. Then, given the quality of the ZOM of the monostatic data, we conclude that monostatic data acquisition has compelling advantages in terms of cost and image quality when compared to bistatic acquisition.

DATA ACQUISITION

The georadar data from LSBB were acquired in March 2011 using an exponentially tapered slot antenna (ETSA) of the Vivaldi type (Yedlin et al., 2010). The ETSA is connected to an agilent vector network analyzer and it operates between 150 MHz to 2 GHz with a noise floor of -120 dB. The monostatic (reflection) data and bistatic (transmission) data are recorded as $a + i\,b$ complex numbers and each recorded number is a stack of 17 monochromatic wave measurements. This system is reported to have a number of outstanding attributes including long depth of resolution due to it's wide bandwidth. Compared to other systems it has a greater dynamic range plus low distortion (Yedlin et al., 2010), and this is achieved with low-noise, low-loss cables and shielding with ultra-wideband absorbers (Yedlin et al., 2010). More details about the system and and acquisition parameters are found in Figure 1 and Table 1. Note, as a prototype, this georadar is quite large as can be seen in Figure 1 (roughly 1 m $\times$ 1 m) and it is quite heavy (about 1/2 a ton) (Yedlin et al., 2010).

Parameter	Detail
Format	Text (real and imaginary parts)
Antennae orientation	Perpendicular to the acquisition direction
Frequency band	100-1500 MHz
Δt	1/3 ns
Maximum t	747 ns (2241 samples)
Offset	monostatic: 0.0 m, bistatic: 0.65 m
Nominal Δx	0.1 m
Actual average Δx	0.926 m
Stack	17 pulses

Table 1. Table of acquisition parameters.

FIG. 1. ETSA antenna and acquisition apparatus in-situ (Yedlin et al., 2010). The width of the central shielding is 25 cm and the distance between the antennae is 65 cm.

DATA PROCESSING

The georadar data are stored as monochromatic signals in a text format as real and imaginary parts. The data are read from this format and then converted to the time domain by IFFT.

Following conversion to time, the first stage of processing is designed to remove a programmed time delay and a source-multiple pulse. The delay is used to avoid direct arrival energy, and the multiple is internal to the source antenna (Yedlin et al., 2010). The time delay is estimated through cross-correlation with a pilot trace (the mean-trace) where we assign $t = 0$ to the maximum amplitude lag and then time-shift the data accordingly. The multiple pulse is very high amplitude but it has the property that it is present on all georadargrams. This noise source can be estimated by a stack of all traces. The signal trace that results is then subtracted from each trace individually and we refer to this as *mean-trace subtraction* (Yedlin et al., 2010). Mean-trace subtraction penalizes horizontal reflections and so other noise reduction procedures can be contemplated.

Data with $t = 0$ correction and mean-trace subtraction applied are shown in Figure 2, where Figures 2(a) and 2(b) give the monostatic and bistatic data respectively. (A bandpass filter and a time-variable display gain (amplitude envelope control) are applied for display only.) There is considerable *ringing* apparent in the data below about 30 ns and this appears to be related to five scatterers embedded in a linear event at about 30 ns.

The next stage in processing is to remove the source pulse and correct for attenuation. Georadar is attenuated much more strongly than seismic (see Ferguson and Margrave, this issue), so nonstationary deconvolution (we apply Gabor deconvolution (Margrave et al., 2011)) is a critical procedure here. Data with Gabor deconvolution applied in Figures 3, 3(a) (monostatic), and 3(b) (bistatic). It is clear that, when compared to Figure 2, we have improved the data significantly. A horizontal reflection is now visible at $\sim$ 75 ns, and a steeply dipping reflector is now apparent between 75 and 200 ns. A summary of processing parameters is given in Table(2).

VELOCITY ANALYSIS

Velocity analysis (VA) for imaging was done following data processing. A ZOM-based approach was used where subsurface diffractions were used as indicators*. To reduce noise, a number of frequencies are excluded from the VA procedure - they are found to have very strong amplitudes and contribute *ringing* to the result. Rather than notch-filter the noisy parts of the spectrum they are simply not used as part of the ZOM imaging-condition step - they do not contribute to the migration output. A table of frequencies and VA parameters is given in Table 3.

For the near-surface, ZOM of the monostatic data was done using numerous test values for velocity $0.15 \times c \leq \alpha \leq 0.25 \times c$ m/s where $c = 3 \times 10^8$ m/s (half velocity) For the deeper section (below 5 m) ZOM was parameterized with $0.1 \times c \leq \alpha \leq 0.3 \times c$ m/s. This

*Gazdag ZOM (Gazdag, 1978) is used where constant lateral velocity is assumed.

Process	Detail
Read spectra from text format	
Convert $(x, \omega) \rightarrow (x, t)$	
Determine $t = 0$	Maximum lag of mean-trace auto-correlation
Mean-trace subtraction	
Gabor deconvolution	`twin`=12.5 ns `tinc`=4/3 ns `tsmo`=50 ns `fsmo`=650 MHz `hsmo`: hyperbolic `stab`=0 `phase`: minimum `gdb`=60
Bandpass filter (display only) (minimum phase)	120-150-900-1500 MHz
AEC (display only)	window width: 110 ns

Table 2. Table of processing parameters. The bandpass filter and AEC scaling are applied for display only.

larger range of values for α was necessary as there are fewer obvious diffractors below 5 m when compared with the near surface. A summary of velocity analysis parameters is given in Table 3.

VA in the nearsurface

ZOM for the monostatic data are shown in Figure 4. Four point scatterers at 1 m depth are somewhat *under-focused* for $\alpha = 17.5\% \, c$ (Figure 4(a)). For $\alpha = 22.5\% \, c$ the diffractors are somewhat *over-focused* (Figure 4(c)). Optimal focusing happens for $\alpha = 20\% \, c$ as can be seen in Figure 4(b) and this value is assigned for α in the upper 5 m. Note that there is good noise cancellation in the upper 5 m and interesting detail is apparent.

As a comparison, the ZOM-based VA is performed using the bistatic data. The bistatic data do not conform to the ZOM model so, as might be expected, the diffractors are less-well focused and this can be seen in Figure 5. Overall, there is less noise cancellation and shallow detail that is apparent on the monostatic tests (Figure 4).

VA in the deeper section

For VA below 5 m, ZOM of the monostatic data is done using the optimal velocity of $\alpha = 0.2 \times c$ and a time-section of data is output at $z = 5\text{m}^{\dagger}$. That is, we downward

[†]This time-section is not to be confused with *time migration*.

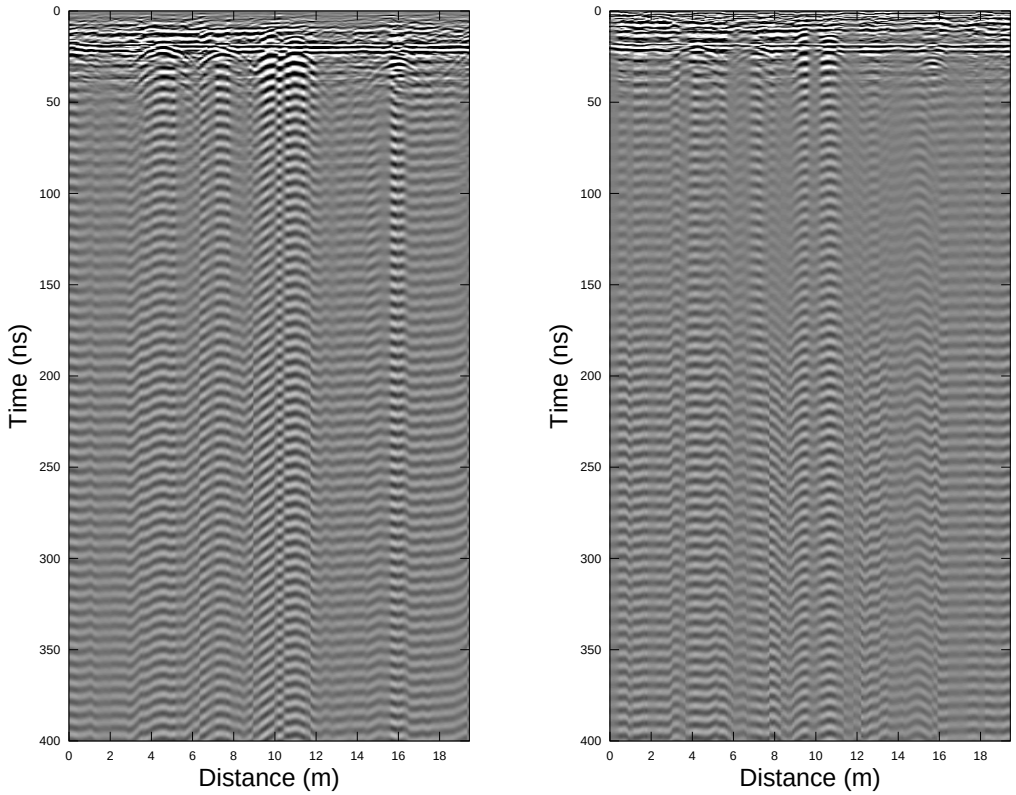

(a) (b)

FIG. 2. Georadar data with mean-trace subtraction applied. a) Monostatic antenna. b) Bistatic antenna.

continue the recorded data to 5 m using ZOM and then output the data in coordinates of $x, t,$ and $z = 5$ m. This time section is then migrated from $z = 5$ m onward using a range $0.1 \times c \leq \alpha \leq 0.3 \times c$ m/s. Some examples of VA for the deeper section using the monostatic data are given in Figure 6. The horizontal reflector between 6 and 8 metres and the dipping reflector (between 6 and 16 metres) are fairly well focused for $\alpha = 27\% \, c$ m/s (Figure 6(b)) and they are less well focused for the bounding values $20\% \, c$ and $29\% \, c$ (Figures 6(a) and 6(c)). Again for comparison, an identical VA for the bistatic data is given in Figure 7. The images are much noisier and the shallow reflector (between 6 and 8 m) is almost completely obscured.

IMAGING

ZOM is applied to the monostatic and the bistatic data, and those images are compared to PSDM of the bistatic data in Figure 8 (for the shallow section) and Figure 9 (for the deeper section) and the corresponding parameters for imaging are given in Table 4. Note, PSDM is done using twice the half velocities. The shallow images for monostatic ZOM and bistatic ZOM are given in Figures 8(a) and 8(b) respectively (they are Figures 4(b) and 5(b) repeated), plus bistatic PSDM in Figure 8(c). Not that the bistatic PSDM appears to have slightly better focusing and more event definition that the monostatic ZOM, and it is much better than the bistatic ZOM.

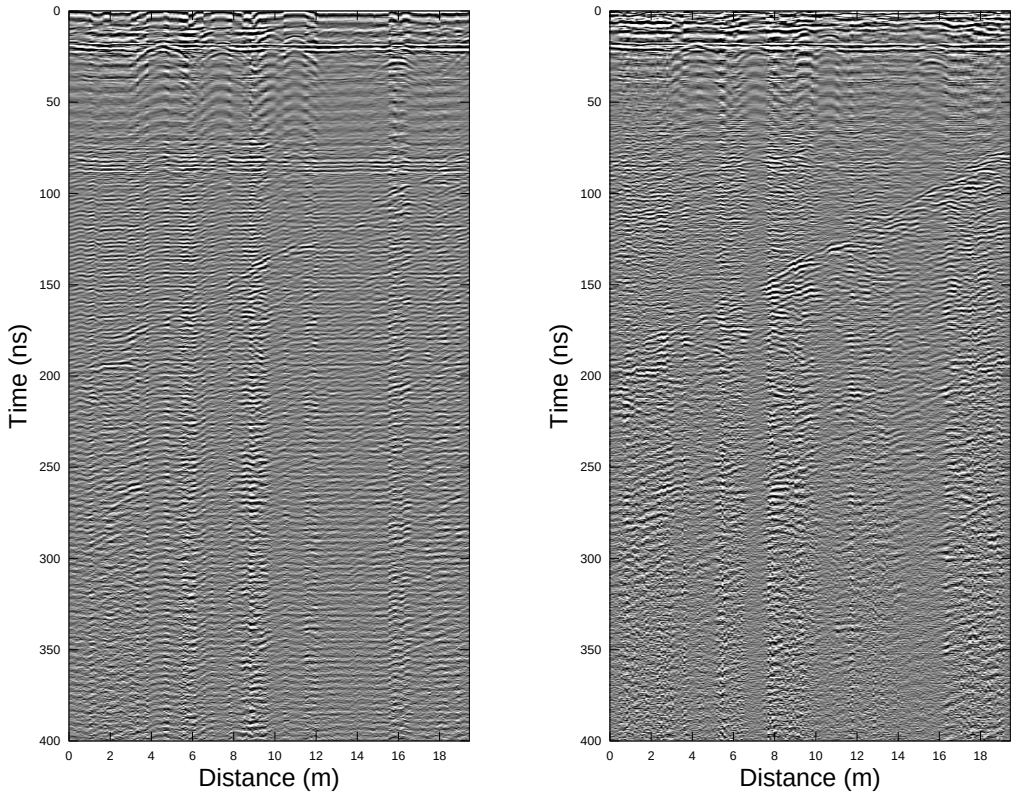

(a) (b)

FIG. 3. Georadar data with mean-trace subtraction plus Gabor deconvolution applied. a) Monostatic antenna. b) Bistatic antenna.

Images for the deeper section are given in Figure 9, where 9(a) is the monostatic ZOM and 9(b) is the bistatic ZOM, with the bistatic PSDM given in Figure 9(c). Though perhaps the dipping event is not as well resolved by bistatic PSDM as in the monostatic ZOM, PSDM may actually have reduced off line noise that might have a contaminating effect on the monostatic ZOM. Both the monostatic ZOM and bistatic PSDM are superior in image resolution and noise reduction compare to bistatic ZOM.

Computational cost

Our ZOM is based on Gazdag (1978) and so we estimate it's cost as $\propto M \log_2 M$ for each migrated frequency and where M is the number of traces. Here, the number of traces is 223 and we zero-pad this to $M = 256$ for ZOM and so cost is $\propto 2048$ per frequency. We estimate cost for our PSDM by similar reasoning. For PSDM of a single bistatic trace, we first insert the trace as a column within a zero matrix where the zero columns around the trace act a padding. We then PSDM migrated each of the padded traces and then sum them all into an image. We found that $N = 128$ was a sufficient number for PSDM of each trace for a cost per trace of $N \log N$ for each frequency. The process is then repeated for each of M traces. If we assume that here $M = 223 \sim 256$ then the relative cost of PSDM over ZOM is $\propto N \log_2 N / \log_2 M$ or a factor of about 100.

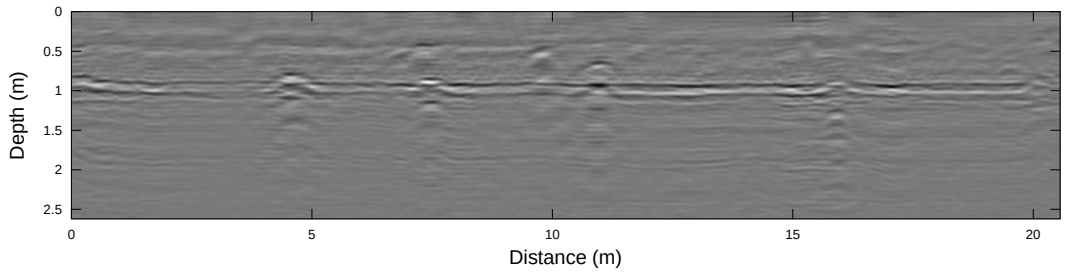

(a)

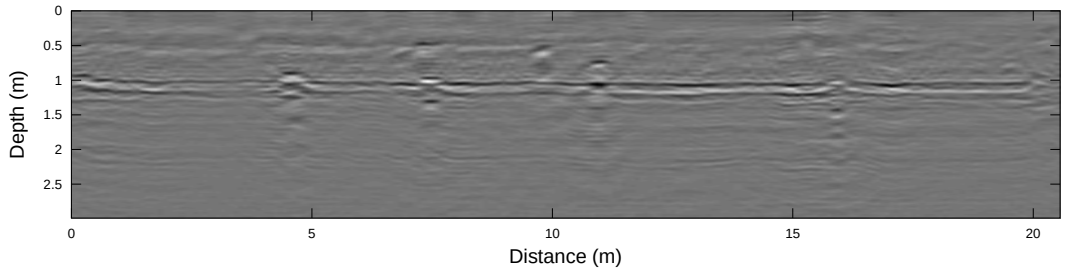

(b)

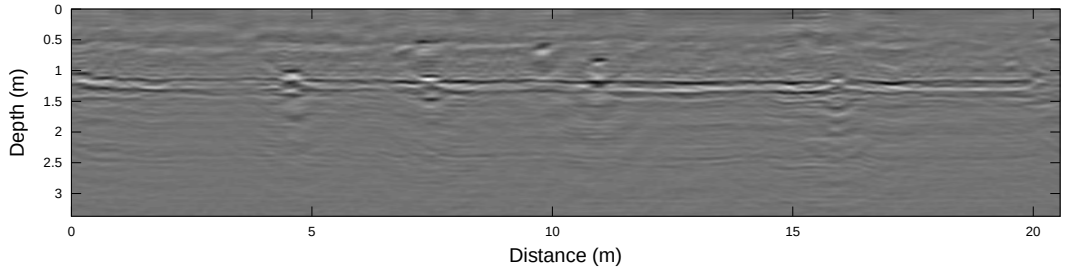

(c)

FIG. 4. Velocity analysis of the near surface by zero-offset migration (ZOM). a) ZOM velocity $\alpha = 0.175 \times c$, where $c = 3 \times 10^8$ m/s. b) $\alpha = 0.2 \times c$. c) $\alpha = 0.225 \times c$.

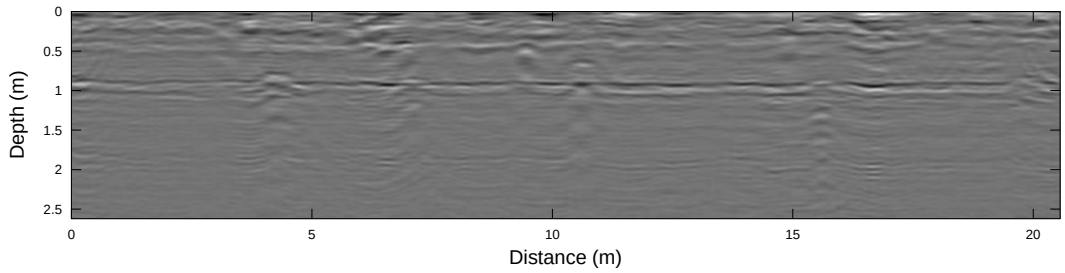

(a)

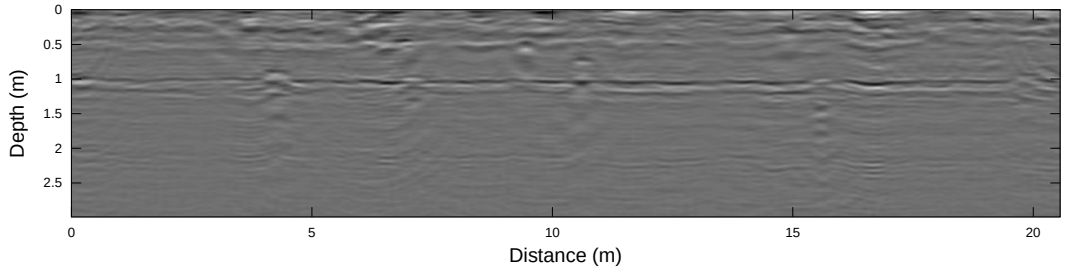

(b)

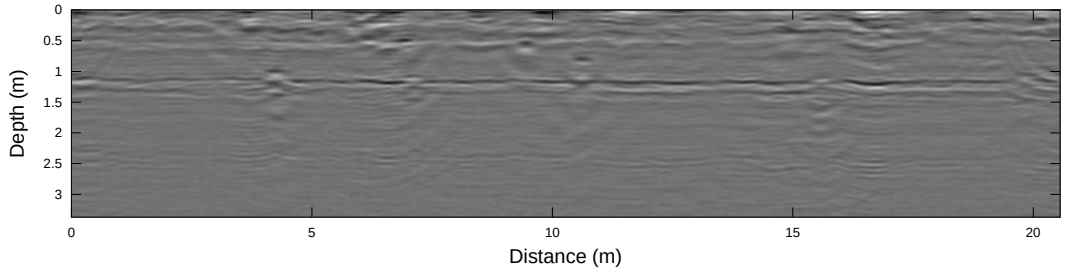

(c)

FIG. 5. Shallow images from ZOM of the bi-static data for comparison with ZOM of the monostatic data (Figure 4). a) Velocity $\alpha = 0.175 \times c$. b) $\alpha = 0.2 \times c$. c) $\alpha = 0.225 \times c$.

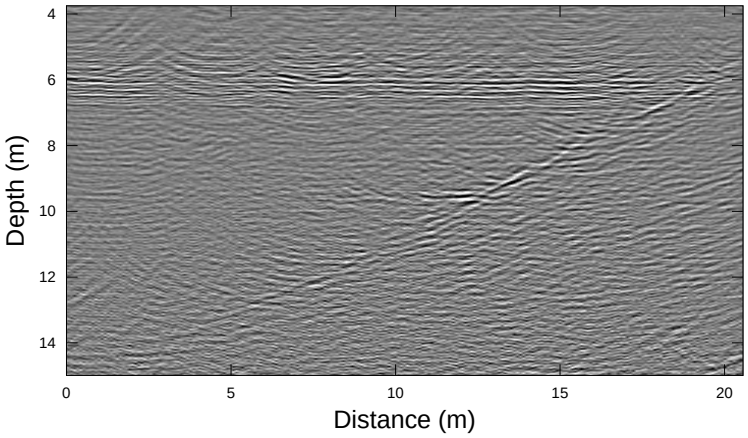

(a)

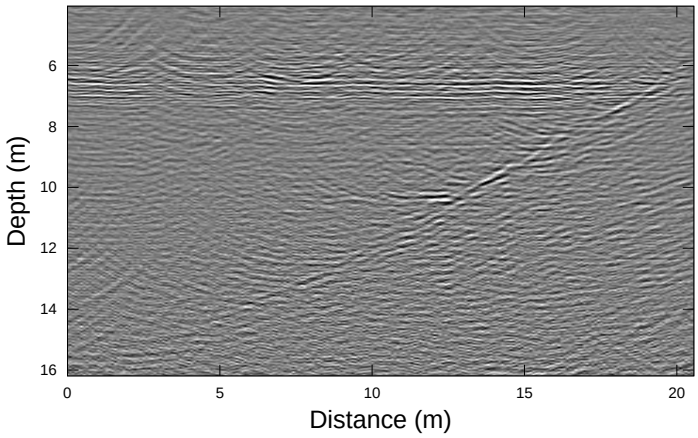

(b)

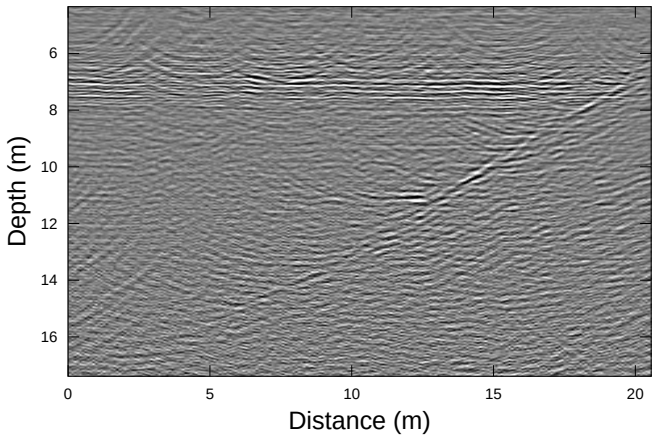

(c)

FIG. 6. VA of the deeper section by zero-offset migration (ZOM). a) Velocity α for ZOM is 0.25 times c. b) $\alpha = 0.27 \times c$. c) $\alpha = 0.29 \times c$.

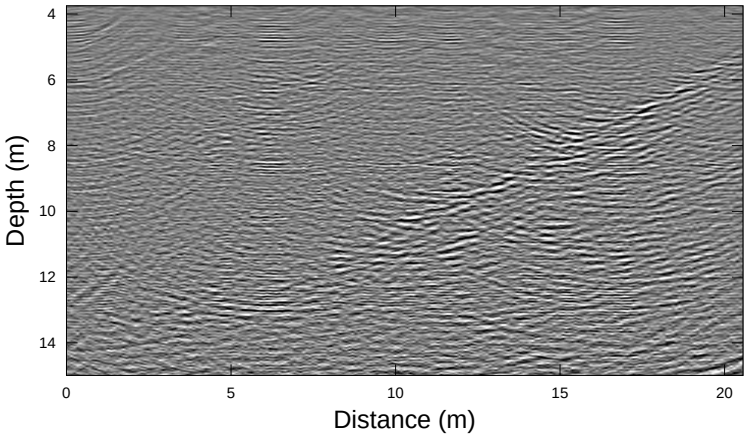

(a)

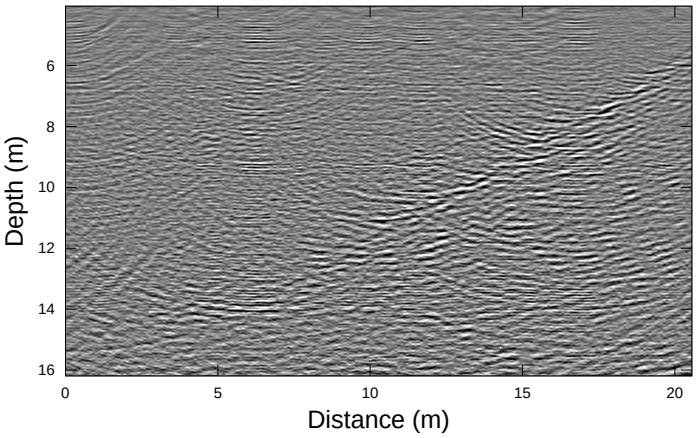

(b)

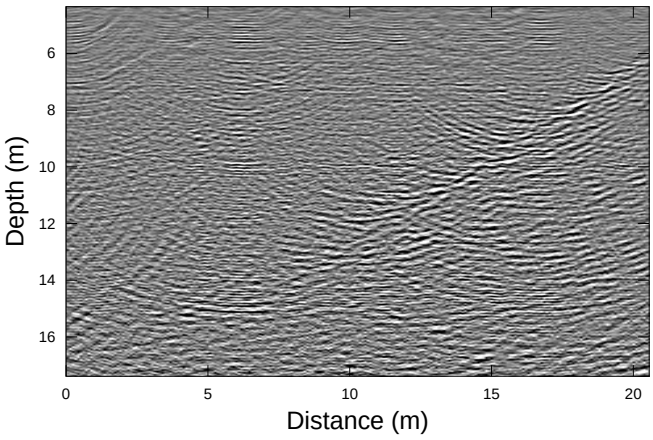

(c)

FIG. 7. VA of the bistatic data for comparison with ZOM of the monostatic data (Figure 6). a) Velocity $\alpha = 0.25 \times c$. b) $\alpha = 0.27 \times c$. c) $\alpha = 0.29 \times c$.

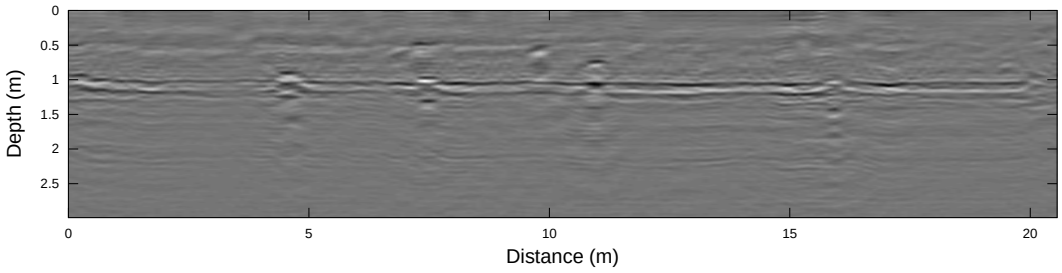

(a)

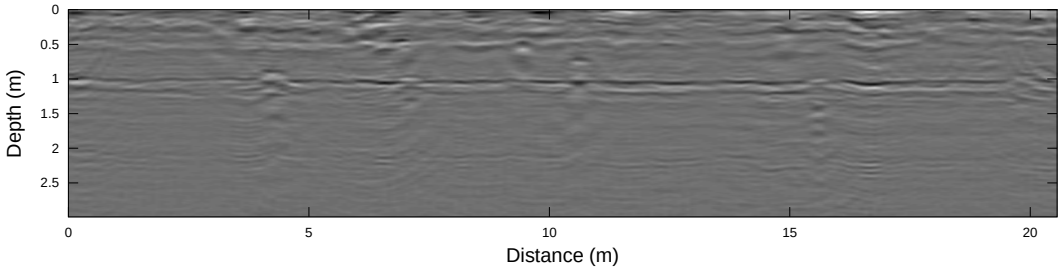

(b)

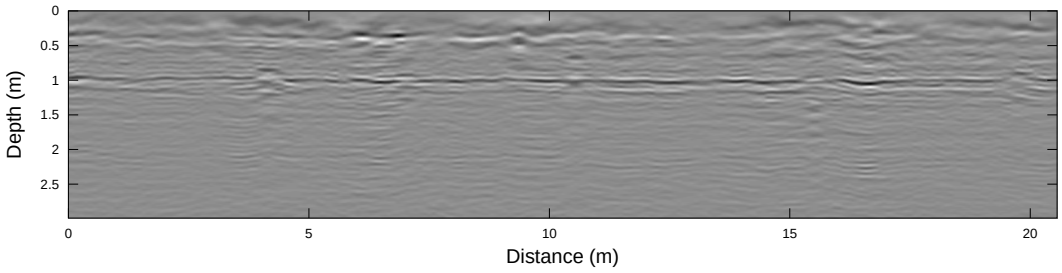

(c)

FIG. 8. Images of the near surface. a) ZOM of monostatic. b) ZOM of bistatic. c) PSDM of bistatic.

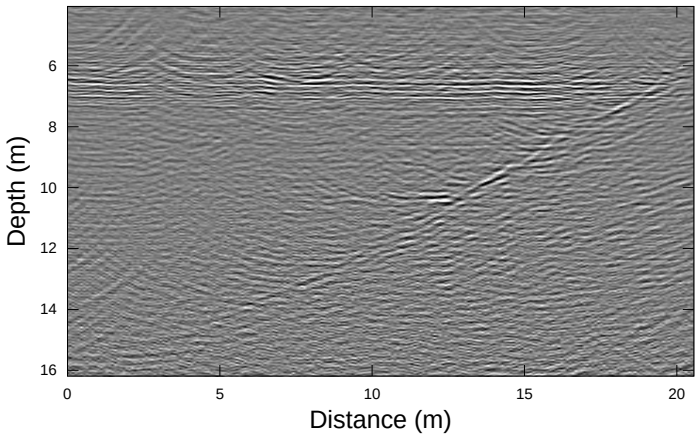

(a)

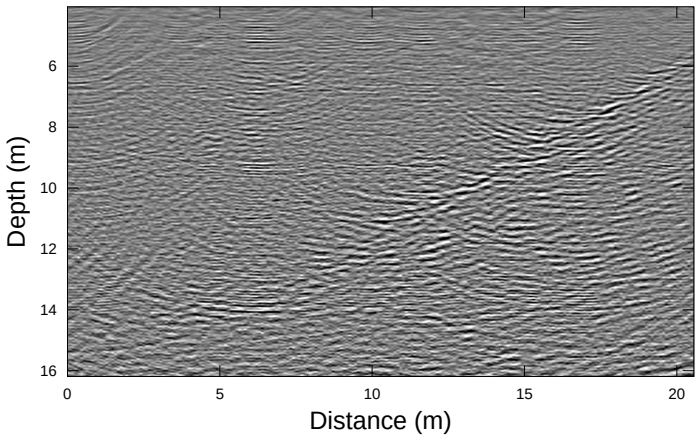

(b)

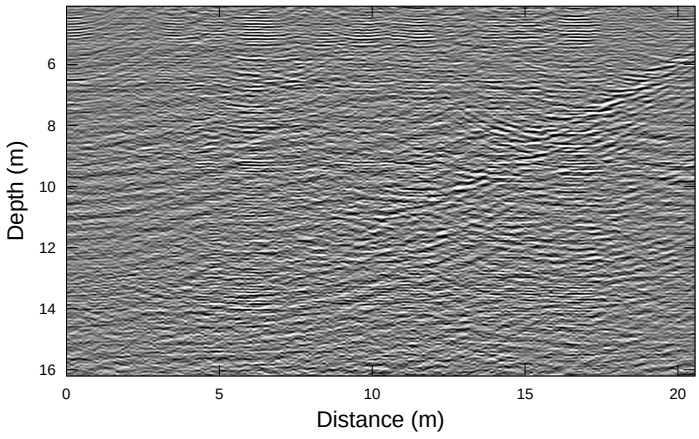

(c)

FIG. 9. Images of a dipping structure. a) ZOM of monostatic. b) ZOM of bistatic. c) PSDM of bistatic.

Process	Detail
Excluded frequencies	Frequency (MHz) 270 MHz 284 MHz 415 MHz 432 MHz 535 MHz 555 MHz
ZOM (monostatic) Gazdag $v\,(z)$	Depth range (m), Velocity (% *c*) 0-5, 15-25 5-15, 1-30
Bandpass filter (display only) (minimum phase)	120-150-900-1500 MHz
AEC (display only)	window width: 110 ns

Table 3. Table of velocity analysis parameters used with monostatic data. The excluded frequencies are not included in the *imaging condition* of ZOM. Test velocities are in %c where $c = 3 \times 10^8$ m/s. Note, all α values quoted are "half velocities" as in ZOM applications. For PSDM they are doubled.

CONCLUSIONS

We present a comparison of true zero-offset migration (ZOM) and prestack depth migration (PSDM) for georadar data. The true ZOM process is enabled by the acquisition of monostatic georadar data within a single source / receiver antenna and these data are compared to imaging results from conventional bistatic data that are acquired simultaneously. The monostatic and bistatic data are first processed to remove source multiple effects that are internal to the acquisition system and then Q attenuation compensation is achieve using Gabor deconvolution. In imaging, we find that ZOM of the monostatic (true coincident source-receiver) data results in comparable images relative to PSDM of conventional bistatic data. We find also that for our small dataset, PSDM is about 100 $\times$ more expensive that ZOM but that the image quality is probably not that equivalently better. Geologically, we find that a shallow zone between 0 and 5 m depth focusses using a half velocity of 20 % of c (20 % the speed of light in a vacuum) or a true velocity of 40 % c. In the deeper section, we find that the half velocity is 27 % c or a true velocity of 54 % c.

ACKNOWLEDGEMENTS

We wish to thank the staff and sponsors of CREWES for their support. We also thank NSERC for their support of this work through CRD grant CRDPJ 379744-08.

REFERENCES

Ferguson, R. J., A. Pidlisecky, and C. Rowell, 2010, Shot record depth migration of georadar: CREWES Research Report.

Gazdag, J., 1978, Wave equation migration with the phase-shift method: Geophysics, **43**, 1342–1351.

Process	Detail
Excluded frequencies	Frequency (MHz) 270 MHz 284 MHz 415 MHz 432 MHz 535 MHz 555 MHz
ZOM (monostatic & bistatic) / PSDM (bistatic) Gazdag $v\,(z)$	Depth range (m), Velocity (% *c*) 0-5, 20 5-35, 27
Bandpass filter (display only) (minimum phase)	None
AEC (display only)	None

Table 4. Table of ZOM and PSDM parameters. ZOM is applied to both the monostatic and bistatic data, and PSDM is applied to the bistatic data. The excluded frequencies are not included in the *imaging condition* of ZOM and PSDM. Migration velocities are in %c where $c = 3 \times 10^8$ m/s. No bandpass filter or scaling is applied.

Margrave, G. F., M. P. Lamoureux, and D. C. Henley, 2011, Gabor deconvolution: Estimating reflectivity by nonstationary deconvolution of seismic data: Geophysics, **76**, W15–W30.

Yedlin, M., G. Sénéchal, D. Rousset, N. Fortino, J. Dauvignac, S. Gaffet, T. Monfret, and C. Pichot, 2010, Comparative study using an uwb measurement system and a ramac gpr system for subsurface imaging of the vaucluse karst aquifer: Wireless Information Technology and Systems (ICWITS), 2010 IEEE International Conference on, 1 –4.